

Emergence of Spatio-Temporal Patterns in Neuronal Activity*§

Iris Haalman and Eilon Vaadia

Department of Physiology, Hadassah Medical School, and The Center for Neural Computation, The Hebrew University, POB 12272, Jerusalem 91120, Israel

Z. Naturforsch. **53c**, 657–669 (1998); received April 27, 1998

Neuronal Activity, Emergence of Spatio-Temporal Patterns

This paper explores if dynamic modulation of coherent firing serves cortical functions. We recorded neuronal activity in the frontal cortex of behaving monkeys and found that temporal coincidences of spikes firing of different neurons can emerge within a fraction of a second in relation to the animal behavior. The temporal patterns of the correlation could not be predicted from the modulations of the neurons firing rate and finally, the patterns of correlation depend on the distance between neurons. These findings call for a revision of prevailing models of neural coding that solely rely on firing rates. The findings suggest that modification of neuronal interactions can serve as a mechanism by which neurons associate rapidly into a functional group in order to perform a specific computational task. Increased correlation between members of the groups, and decreased or negative correlation with others, enhance the ability to dissociate one group from concurrently activated competing groups. Such modulation of neuronal interactions allows each neuron to become a member of several different groups and participate in different computational tasks.

Introduction

Most of the electrophysiological studies to date have recorded the activity of single neurons individually, assuming that cortical computations are properly represented by the firing rates of single neurons. The experimental results provided ample evidence that the firing rate of single neurons in peripheral and central nervous system can, in many cases encode accurately sensory information. Thus at one extreme, stands the view that the sensory system is designed to represent a given entity by a minimal number of active neurons. This is the *sparse coding* or *cardinal cell* hypothesis (see Barlow, 1972; 1992). Another approach to rate-code assumes that the accuracy of the single unit

firing-rate is not satisfactory. Thus, encoding is achieved by the combined firing rate of a selected population of neurons. The most typical example of this approach is the “*population rate codes*” of movement trajectory (Sparks *et al.*, 1976; Georgopoulos *et al.*, 1986). Recent studies demonstrated that the population rate code can be generated rapidly before the movement is executed, it can code for spatially directed attention (Wise *et al.*, 1996) and can rotate on a short time scale, within 10–20 ms (Georgopoulos *et al.*, 1989; Schwartz, 1993; 1994). At this stage, the mechanism of generation of population rate codes is unknown. Several neural network models, which address this issue, emphasize the role of adjustable connectivity between the neurons. It has also been shown that *coherent activity* in groups of neurons can be represented as “*attractors*” in neural network models (Lukashin and Georgopoulos, 1993; Seung and Sompolinsky, 1993; Salinas and Abbott, 1994) and serve in organizing functional groups of neurons (von der Malsburg, 1981; Rotter and Aertsen, 1998; this issue, pp. 686–690).

Electrophysiological studies support the notion that coherent activation of groups of interacting neurons is involved in neuronal computation. Examination cortical activity by optical imaging, recordings of EEG, local field potentials, multi-unit activity and multiple spike-trains of single neurons

* This communication is a contribution to the workshop on “Natural Organisms, Artificial Organisms, and Their Brains” at the Zentrum für interdisziplinäre Forschung (ZiF) in Bielefeld (Germany) on March 8–12, 1998.

§ This manuscript is based on the chapter: Spatiotemporal patterns of neuronal activity in the frontal cortex of the behaving monkey: evidence for dynamic cell assemblies. In: The Association Cortex – Structure and Function (Skata H., Mikami A. and Fuster J. M., eds.). Harwood Academic Publishers 1997.

Reprint requests to Ph.D. E. Vaadia.

Fax: 972-2-643 9736.

E-mail: eilon@hbf.huji.ac.il.



demonstrated coherent activation in local cortical circuits and even between distant neurons located several millimeters apart (Eckhorn *et al.*, 1988; Gray *et al.*, 1989; Krüger, 1990; Engel *et al.*, 1991; Nelson *et al.*, 1992; Sanes and Donoghue, 1993; Murthy *et al.*, 1994; Desmedt and Tomberg, 1994; Arieli *et al.*, 1995; Murthy and Fetz, 1996 and many others).

Interactions among single neurons were commonly investigated by crosscorrelation analysis of simultaneously recorded pairs of spike trains, especially when direct measurement of the synaptic potentials is impossible. It was usually assumed that crosscorrelograms reflect the underlying synaptic connectivity (e.g. Gerstein and Perkel, 1969; Moore *et al.*, 1970; Toyama *et al.*, 1981; Ts'o *et al.*, 1986; Fetz *et al.*, 1991). However, the anatomy of the cortex indicates that neurons are interconnected in very large networks (Braitenberg and Schüz, 1991). This implies that the crosscorrelogram between any two neurons reflects the net effect of direct and indirect synaptic connections between them, as well as contributions from their connections with the remainder of the network. Therefore, recent studies emphasize the interpretation of crosscorrelation results in terms of functional (or effective) coupling between neurons, characterizing the instantaneous organization of the cortical network (Aertsen *et al.*, 1989; Ahissar *et al.*, 1992a,b).

Various types of *spatiotemporal firing patterns* were observed. The findings include synchronized oscillations non-oscillatory correlations and re-occurring patterns of spike firing with millisecond precision. Spatiotemporal patterns are often rapidly modulated in relation to presentation of stimuli or to the initiation of movements with very precise timing or loose timing (Eckhorn 1988; Gray *et al.*, 1989; 1992; Engel *et al.*, 1991; Allum *et al.*, 1982; Kwan *et al.*, 1987; Krüger and Aiple, 1988; Smith and Fetz, 1989; Nelson *et al.*, 1992; Vaadia and Aertsen, 1992; Abeles, 1982; 1993a,b; Ahissar *et al.*, 1992a; Vaadia *et al.*, 1995a). On the basis of these and other findings, it was suggested that coherent activity may be used to “bind” disparate neuronal activities, representing separate perceptual elements, into a functional assembly, representing a global precept (von der Malsburg, 1981; Gray *et al.*, 1989; Schillen and König, 1994; Abeles *et al.*, 1993a; Bienenstock and German,

1993. For a recent review and discussion on alternatives for bindings see also the chapter by Pieter Roelfsema, 1998: this issue, pp. 691–715).

At present it can not be decided whether neural encoding consists solely on one of the above options, or whether the different codes and computational mechanisms coexist. Combined investigations of the relations between neuronal interactions, single unit firing rate and the animal behavior is necessary to approach these questions. To do that it is essential to record and isolate the activity of several neurons in a behaving animal. This was the approach we took in the study described here. Our working strategy does not attempt to compare the amount of information carried by *rate code* versus *spatiotemporal code*. Rather we examine two phenomena (modulation of firing rate and modulation of interactions) and attempt to evaluate their mutual relations and its relevance to the animal behavior.

Recording Procedures and Data Analysis Tools

Two monkeys (*Maccaca mullata*, female, 3–4 kg) were trained to perform a spatial delayed response task (Fig. 1). Trials were initiated when the monkey touched a central key and a central red light was turned on (*ready*). After a variable delay (3–6 s), one of two target keys was illuminated for 200 ms (*spatial cue*).

After a delay of 1–32 s, the central red light was dimmed (*trigger*) instructing the monkey to select the appropriate behavioral response. In one paradigm (GO) the monkey was rewarded for releasing the center key within 0.6 s (RT = reaction time) after the trigger signal, and touching the correct target key within the next 0.6 s (MT = movement time). In the second paradigm (NO-GO) the monkey was rewarded for continuing to touch the center key for at least 1.2 s after the trigger. Special peripheral lights (*“mode toggle”*) instructed the monkey to switch paradigms every four correct trials. When the monkey was over-trained a recording chamber was placed above a hole in the skull, to allow for electrode penetration to a large area in the frontal cortex around the arcuate sulcus (Fig. 2) and recording sessions begun. In each session we recorded simultaneously neuronal activity during performance of 400–800 correct trials with 100–200 alternations between the two behav-

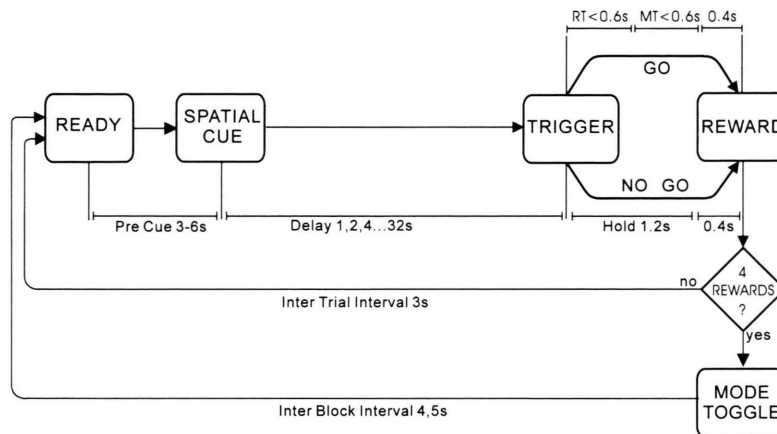


Fig. 1. The spatial delayed-response task. Trials were initiated when the monkey touched a central key and a central red light was turned on ("ready"). After a variable delay (3–6 s), one of two target keys was illuminated for 200 ms ("cue"). After a delay of 1–32 s, the central red light was dimmed ("trigger") instructing the monkey to select the appropriate behavioral response. In one paradigm ("GO") the monkey was rewarded for releasing the center key within 0.6 s (RT = reaction time) after the trigger signal, and touching the correct target key within the next 0.6 s (MT = movement time). In the second paradigm ("NO-GO") the monkey was rewarded for continuing to touch the center key for at least 1.2 s after the trigger. Special peripheral lights instructed the monkey to switch paradigms every four correct trials.

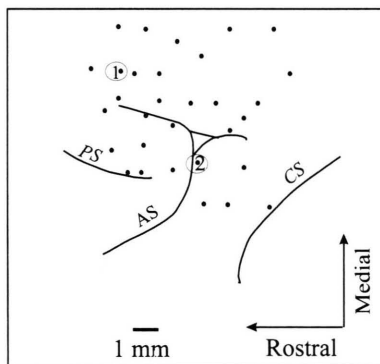


Fig. 2. Surface map of recording sites. The neurons of the examples in figures 4 and 5 were recorded in sites 1 and 2 correspondingly. The figure depicts a portion of the frontal cortex around the arcuate sulcus. (AS). Part of the principal sulcus (PS), the central sulcus (CS) and the superior diple (SD) are also shown.

ioral paradigms. Six microelectrodes (glass-coated tungsten, 0.2–1.5 M Ω impedance) were inserted into the cortex in a circular array, with 500–1000 microns inter-electrode distance. Spike-sorters were utilized to isolate the activity of 1–3 single units from each electrode. Typically, we recorded in each session 4–8 well-isolated units and 6–10 clusters with a mixture of 2–3 spike-shapes in each

cluster. Eye movements were monitored by Ag–AgCl cup-electrodes. The locations of electrodes tracks in the cortex were reconstructed by standard histological techniques. Raster displays and peri-stimulus time histograms were used to examine neuronal activity. The temporal firing patterns and interactions between neurons were first studied by autocorrelograms and crosscorrelograms. Unfortunately, this conventional correlation analysis is not an adequate tool to study the temporal evolution of firing patterns and coherent firing, since it measures the time-averaged rate of near-coincident spikes over a long time interval, typically on the order of several seconds or minutes. It is for this reason that we also applied dynamic crosscorrelation analysis, by computing the **Joint Peri-Stimulus Time Histogram (JPSTH)**. This analysis was used to highlight the detailed time structure of firing correlation between two neurons and its time-locking to a third event (such as the onset of a stimulus). The method is briefly described below, for more details see Aertsen *et al.* (1989).

The starting point for our considerations is the Joint Peri Stimulus Time Scatter Diagram (Gerstein and Perkel, 1969; 1972). Figure 3a presents a two-dimensional matrix, showing how

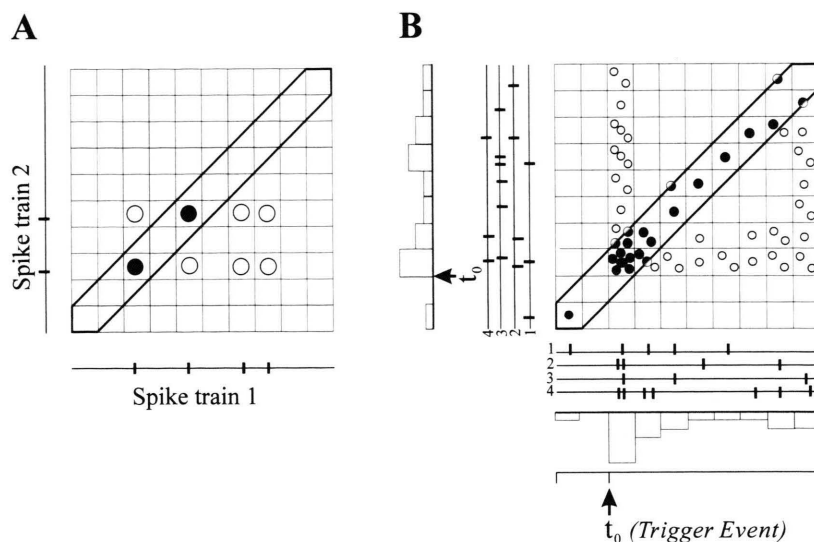


Fig. 3. Constructing the Joint PST Histogram for simulated spike trains. **A:** Contribution of one time segments to the correlation matrix (10×10 bins). Spikes of one neuron are displayed as small vertical lines under the x -axis of the matrix. Spikes of the second unit are displayed along the y -axis. The time of a trigger event is marked as t_0 . Each circle in the matrix represents one occurrence of a “coincidence” of a given delay within the selected time segment. If the two neurons fire at the same time (within the bin size) the event is marked by filled circles (“true-coincidences”). Note that these events always fall on the main diagonal (shaded in gray). **B:** Constructing a JPST matrix for four segments (numbered 1–4) of two spike trains around t_0 . The simulated spike trains were set to demonstrate typical features of the “raw JPST”: 1. Vertical and horizontal strips of denser counts (reflecting modulation of firing rates of the neurons) 2. Diagonal strip of black circles representing a tendency of the neurons to fire in synchrony. The PSTs of the two simulated spike trains are shown under the x -axis and along the y -axis (gray histograms) or the initiation of a movement) and to examine its relation to the firing rate of the two neurons.

spikes which occurred around the time of presentation of a trigger event (e.g. stimulus) are treated. Spikes firings of one neuron are displayed along the x -axis and the firings of the other neuron are displayed along the y -axis. The time of firing of the two neurons are measured relative to the time of the trigger (which is set to t_0). Counts are entered into bins of the matrix at positions corresponding to the time-combination of the firings. For example, the filled circles represent points in time, at which both neurons fired simultaneously. We call such occurrences “true coincidences”. These always appear on the main diagonal (marked in gray). Handling repeated presentations of the same triggers (repeated occurrences of the same stimulus or behavioral event, such as initiation of a movement) is shown in Fig. 3B. Four such “trials” are shown (marked 1–4). Again, all trials are aligned such that the time of occurrence of the trigger event is set as t_0 . The scatter diagram shows increased point densities parallel to the axes, (empty circles) representing stimulus/beh-

avior related firing modulations of one or both neurons. There may also be increased point densities along and near the main diagonal of the plane (shaded in gray), representing the epochs of increased amount of true-coincidences (filled circles). Averaging of the number of spikes firing of each neurons across all trials, generates the ordinary single neuron PST histograms (gray histograms along the x - and y -axes). Similarly, the near coincidence counts (along the diagonal) can be displayed as a coincidence time histogram (not shown in Fig. 3). Finally, summation of each of the diagonals, from bottom left to top-right produce the conventional crosscorrelogram (not shown in Fig. 3).

These are all ‘raw’ measurements, i.e. they do not take into account the effects of possible stimulus- or behavior-locked modulation of the two individual neuron firing rates. Time-locked changes in these rates through the repeating cycle would necessarily lead to corresponding changes in the near-coincidence rates. For the present purpose

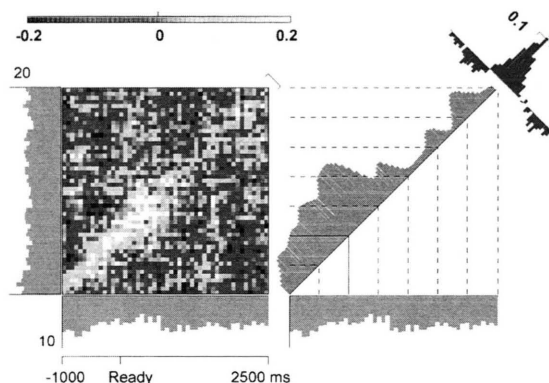
this is an uninteresting ‘background’ effect that we would like to eliminate from the correlation in order to study those components which indicate temporal changes in the underlying neuronal interaction which reflect the ‘effective’ or ‘functional coupling’ between the neurons involved. Aertsen et al devised the appropriate normalizing calculations to distinguish between independent modulations of firing rates of the two neurons from inter-neuronal interactions (for details see Aertsen *et al.*, 1989; Palm *et al.*, 1988). The normalization involves subtracting a “PST predictor” from each bin in the JPST matrix. The predictor of a given bin ij in the matrix is computed by multiplying the values of the two corresponding bins in the individual PST histograms: $\lambda_1(i) \cdot \lambda_2(j)$ where λ_1 and λ_2 are the firing rates of neuron 1 and neuron 2. Finally, the result of the subtraction is normalized by dividing each bin by the product of the standard deviations of the corresponding PST bins. Thus, the amount of excess of coincidences in each bin is expressed as a correlation coefficient (for the selected bin size). These values can be displayed as histogram (*coincidence-time-histogram*: CTH). The CTH is of particular interest here since it represents the stimulus time-locked average of near-coincident firing of the two neurons in the same sense that the ordinary PST-histogram represents the stimulus time-locked average of firing by each individual neuron. The CTH depicts only coincidences of firing which may result from interactions among neurons. From here on we use the term **CTH** for the corrected and normalized coincidence time histograms. These are shown in Figs 4, 5 as diagonal histograms.

To conclude, the normalized JPSTH depicts the excess of spike correlation above the expected correlation due to co-variations of firing rates and express them as correlation-coefficients. Thus, the normalized JPSTH reflects the net effect of direct and indirect interactions of the two neurons. Using this computational tool we could examine rapid, stimulus- or behavior-related changes in the interactions between two observed neurons.

Behavior-Related Modulations of Firing Correlation

We examined the temporal patterns of correlated activity of pairs of neurons in relation to the

A. GO PARADIGM



B. NO-GO PARADIGM

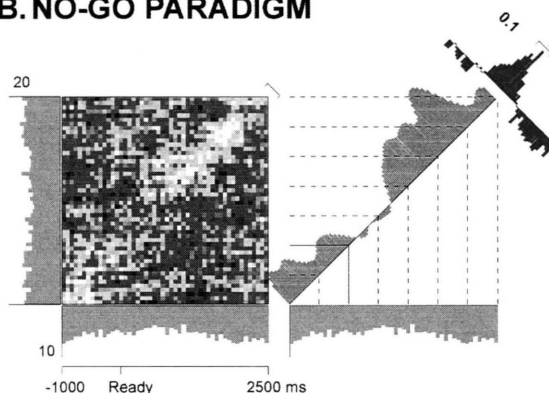


Fig. 4. Dynamic modification of correlated firing of two frontal cortex neurons in relation to a visual stimulus (“ready” signal) as revealed by the normal JPSTH. The left half of each plot (A and B) shows the correlation JPST matrix (gray-scale shown in A), and two ordinary PST histograms along the x-axis (unit 1, full scale: 10 spikes/s) and the y-axis (unit 2, full scale: 20 spikes/s). Binwidth: 70 ms (PST histograms) and 70 ms × 70 ms (matrix). The right half of each JPSTH shows the coincidence-time histogram (CTH, full scale is: 0.15) and the crosscorrelogram (full scale: 0.1). The CTH was smoothed by convolution with a gaussian ($\sigma = 140$ ms, two bins). The PST of unit 1 is duplicated along the x-axis of the right side for clarity. The distance between the grid lines is 500 ms. The onset of the ready signal is marked by solid lines in the grid. A: JPSTH constructed from 221 GO trials, with 4414 spikes of unit 1 and 10,121 spikes of unit 2. Observe a gradual build-up of excess correlation, which starts before the onset of the ready signal, reaches a peak 400 ms after the signal and then decays. B: JPSTH constructed from 194 NO-GO trials for the same neurons (unit 1: 3764 spikes; unit 2: 8715 spikes). Note the different evolution of the correlation in comparison to A (modified from Vaadia *et al.*, 1995a).

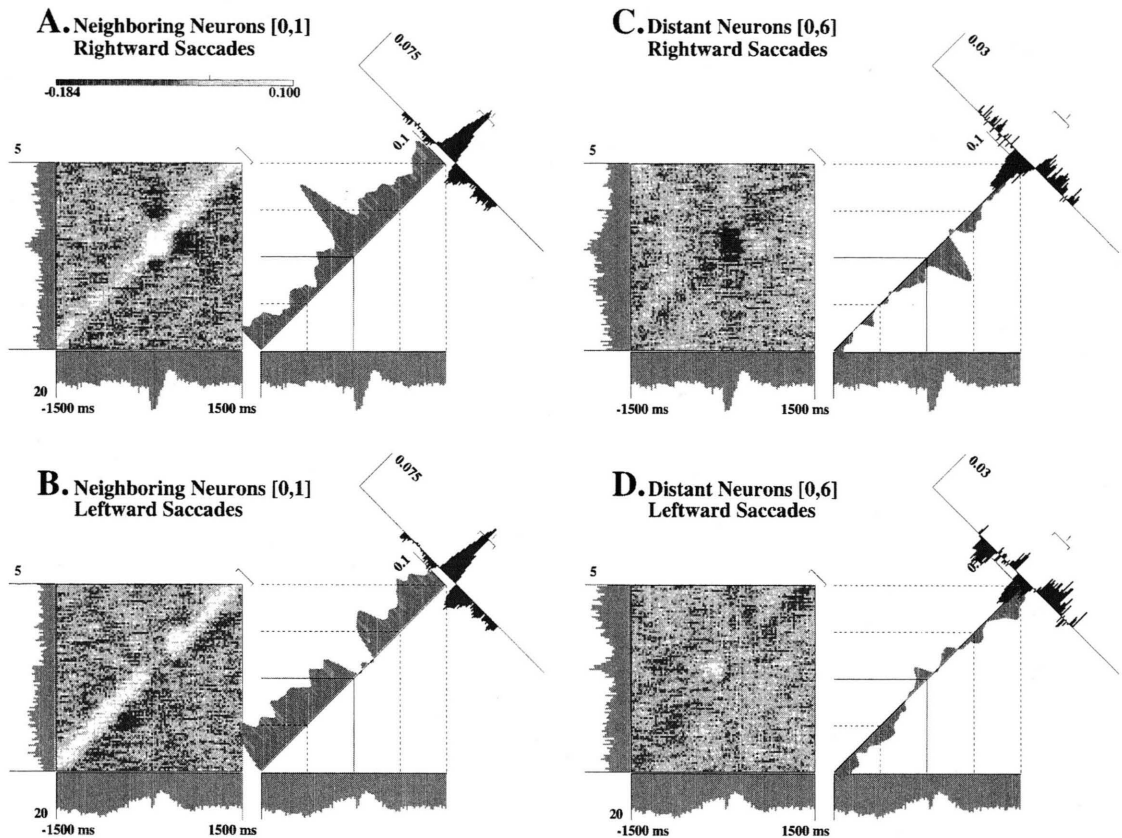


Fig. 5. Dynamic modification of correlated firing between frontal cortex neurons in relation to the onset of saccadic eye movements. A, B: JPSTHs for units 0 and 1 that were recorded by the same microelectrode (neighboring neurons [0,1]). C, D: JPSTHs for two distant neurons [0,6]. Unit 0 is the same unit shown in A and B. Unit 6 was recorded by another electrode. Note that: 1. The averaged crosscorrelograms for a given pair are similar. However, as shown by the matrix and the coincidence histograms, the dynamics are temporally linked to the saccades and depend strongly on their direction (A vs. B and C vs. D). 2. The correlations between neighboring neurons (A and B) are positive, whereas the correlations between distant neurons are negative (C and D). The normalization and format of the JPSTs are the same as in Fig. 4. Bin size in all plots is 30 ms. The JPSTs around onsets of rightward saccades (A and C) were constructed from 776 saccades, with 33,882 spikes of unit 0 (A and C), 4299 spikes of unit 1 (A) and 6927 spikes of unit 6 (C). The JPSTs around onsets of leftward saccades (B and D) were constructed from 734 saccades, with 32,621 spikes of unit 0 (B and D), 4167 spikes of unit 1 (B) and 5992 spikes of unit 6 (D) (from Vaadia *et al.*, 1995a).

onset of visual stimuli (ready, cue, trigger) and in relation to the motor behavior of the monkey (initiation of arm movements and of saccadic eye movements).

Correlated activity was found in 499 neuronal pairs. The time-averaged crosscorrelogram of these neuronal pairs could have a peak (positive correlation), a trough (negative correlation) or a mixed pattern including both peaks and troughs (compound correlation).

Peaks and troughs were always located near time 0 of the averaged crosscorrelogram, and de-

cayed within tens to a few hundred milliseconds (cf. Figs 4 and 5, red histograms). All 499 neuronal pairs were analyzed in detail by examining the JPST histograms. We found that the dynamic pattern or the strength of the correlation was modified significantly in relation to behavior in 308/499 cases (61%). Examples of such modulations are shown in Figs 4 and 5. Each JPSTH in the figures is composed of four displays: 1. Peri-stimulus time histograms (PST's; horizontal and histograms), depicting the individual firing rate of each of the two neurons 2. A gray-scale normalized

JPST matrix. The amount of excess of coincidences is expressed as correlation coefficients. The “dark” regions represents co-firing at a rate lower than expected for uncorrelated firing, whereas lighter-white represents the highest co-firing rate above the expected rate. 3. The CTH (coincidence-time-histogram) a gray diagonal histogram, showing the temporal evolution of the correlation-coefficient relative to the trigger event; 4. The conventional, time-averaged crosscorrelogram (top-right histogram). We stress again that these JPSTHs were normalized as described above, to distinguish between the contributions of inter-neuronal correlation and the stimulus (or behavior) induced co-variation of single-neuron firing rates. To facilitate the interpretation, we also computed the correlation strength by the measuring the relative deviation of the observed coincidence rate from the expected rate for independently firing neurons. The maximal absolute value of this ratio, measured along the coincidence-time histogram, and expressed as a percentage of the expected rate, was denoted as the ‘maximal modulation depth’.

Figure 4 shows JPSTHs for two neurons in the rostral-premotor cortex (dorso-medial frontal cortex, site 1 in Fig. 2). In this case, the JPSTH reveals behavioral dependent modulation of co-firing that could not be predicted from the individual firing-rates (‘responses’) of the two neurons or from the time-averaged crosscorrelograms.

The two JPSTHs in A and B show the joint activity of these two neurons in the two behavioral paradigms: GO (A) and NO-GO (B). The time scale spans 3500 ms, beginning 1000 ms before the ready signal. During this entire period, the monkey’s hand was touching the central key. The firing rate of one unit does not change throughout the interval, (histogram along the *y*-axis of plots A and B). The firing rate of the second unit shows a weak modulation, with a small decrease following the onset of the ready signal (histogram along the *x*-axis of plots A and B). Moreover, the remarkably similar PST histograms in A and B show no significant difference between the firing rates of both neurons during performance in GO paradigm trials and performance in NO-GO trials. Thus, PST analysis alone would indicate that these two neurons taken individually neither respond to the ready signal, nor contribute to the discrimination between the two behavioral paradigms. Evaluation

of the time-averaged crosscorrelation (histograms on the upper-right of each plot) does not change this inference. Both crosscorrelograms are characterized by a relatively broad peak around the origin. This peak indicates that the probability that each of the two neurons will emit a spike is highest when the other neuron fires a spike as well, and decays with a time constant of about 300 ms (as reflected by the peak width). Comparison of the crosscorrelograms in plots A and B, however, does not reveal any qualitative difference. Thus, the time-averaged correlation does not discriminate between the two behavioral paradigms. The situation is quite different, though, when we examine the dynamics of correlation. The time course of the amount of co-firing contributing to the crosscorrelogram peak is shown along the main diagonal (from bottom-left to upper-right) of the gray-scale matrix. This time course of excess near-coincident firing is emphasized in the diagonal CTH. The most outstanding feature in the top panel (A) is the gradual change of co-firing along the principal diagonal. Co-firing is evident and increasing from the beginning of the selected interval, reaches a peak after the onset of the ready signal (maximal modulation depth = 50%), and then decays to the expected (uncorrelated) level. By contrast, the correlation in the NO-GO condition (B) shows a very different time course. Here, the co-firing decays from the beginning, and reaches the zero-level just after the onset of the ready signal, after which the firing of the two neurons remains uncorrelated for about a second, and finally increases to a high level of correlation. This detailed dynamic analysis indicates that the correlation between these two neurons is strongly modulated and temporally linked to the onset of the ready signal. Moreover, the figure illustrates that the evolution of co-firing is practically opposite in the two behavioral conditions. During performance of the GO paradigm, the co-firing is maximal about 500 ms after the onset of the ready signal; whereas during the NO-GO trials, the co-firing at that time is minimal. We stress that this difference in the evolution of co-firing could not be predicted from the responses of the two neurons alone, nor was it reflected in the time-averaged crosscorrelograms. However, the dynamics of the correlation between these two neurons reveal that they participate in the coding of the sensory event and of the behavioral context.

Correlation Dynamics Depend on Distance between Neurons

Previous studies of visual cortex neurons indicated that the strength and pattern of the time-averaged crosscorrelation may depend on the locations of the two neurons in the cortex (Ts'o *et al.*, 1986; Eckhorn *et al.*, 1988; Gray *et al.*, 1989; 1992; Krüger, 1990).

Figure 5 shows examples of correlation dynamics in two pairs of neurons recorded simultaneously by two microelectrodes in the frontal eye field, near the genu of the arcuate sulcus (site 2 in Fig. 2). The first two neurons, 0 and 1 [0, 1], were recorded by a single microelectrode. The distance between the cell bodies of neurons that can be monitored simultaneously by a single electrode, is estimated at less than 100 microns (Abeles, 1982). Hence, we refer to them as *neighboring neurons*. The second pair [0, 6] consists of one neuron from the first pair (neuron 0) and another neuron (neuron 6) which was recorded by a different electrode, located about 400 microns deeper and 500 microns lateral to the first electrode. Hence, we refer to neurons 0 and 6 as *distant neurons*. Figure 5A, B shows JPSTHs for the neighboring neurons [0, 1].

The top plot (A) shows the JPSTH around the initiation of saccades to the right. The bottom plot (B) shows the JPSTH for the same pair around saccades to the left. The peri-saccade time histo-

grams in the plots along the *x*- and *y*-axes show that in both cases the firing rates of the neurons were modulated before and during the saccades. The peaks of the crosscorrelograms in A and B indicate that, on the average, the amount of correlation between the two neurons is similar in the two conditions. The JPSTH analysis, however, clearly reveals that these time-averaged crosscorrelations are misleading. While the average correlation is indeed constant, dramatic modifications of co-firing occur near the initiation of the saccades; Just as the rightward saccade starts, co-firing increases to its highest level within a few tens of milliseconds (white cluster in the center of the matrix, maximal modulation depth = 110%). The opposite change takes place for saccades in the leftward direction (B), where the correlation decreases to zero (no-correlation) as soon as the eye movement starts. The JPSTHs in C and D show the same analysis for the distant pair [0, 6]. In this case, the average correlation is negative, i.e., the probability that either one of the neurons will fire a spike is lower around the times the other neuron fires. This type of correlation can result from reciprocal effects of correlated inputs to the two cells (while one neuron is excited by the net effect of the correlated inputs, the other is inhibited). Alternatively, it may reflect mutual inhibition between the two neurons. Again, the JPSTH shows that the average correlation is misleading. In fact, the negative correlation is only evident just after the initiation of saccades to the right (C; maximal modulation depth of 70%), and is completely missing around the onset of saccades to the left (D). Identical patterns of correlation dynamics were found between neurons 1 and 6 (not shown). The plots in Fig. 5A, B depict the correlation dynamics between two neighboring neurons that show a modulation of positive correlation. By contrast, the plots in Fig. 5C, D describe modulations of negative correlation, found between two distant neurons.

The distribution of correlation patterns was examined by comparing JPSTHs of neuronal pairs that were recorded by the same electrode, to JPSTHs of neuronal pairs that were recorded by different electrodes. The horizontal distance between two adjacent electrodes in this study was 500 to 1000 microns. Figure 6 summarizes the results of this comparison. The figure illustrates that

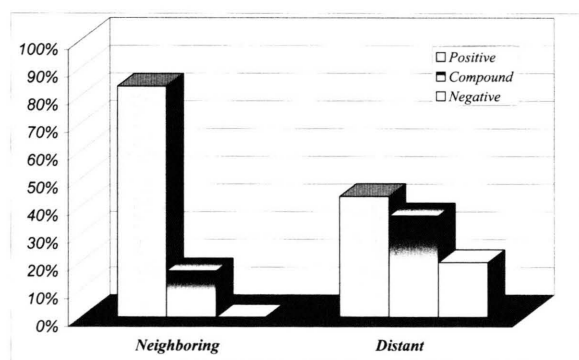


Fig. 6. Distribution of crosscorrelogram patterns in neighboring vs. distant neurons. Positive peaks in most cases characterize Crosscorrelograms between pairs of neighboring neurons. Note that negative crosscorrelograms are completely missing in the population of neighboring neurons. The number of neuronal pairs in each class is given above the bars. The difference between the two populations is statistically significant at a level of 0.001.

positive correlation was observed between distant neurons as well as between neighboring neurons, but more frequently between neighboring ones. By contrast, negative correlation was only found between distant neurons, and never between neighboring ones.

Modulation of Firing Rate versus Modulation of Neuronal Interactions

The excess of coincidences found in this study can be interpreted as the reflection of a process of dynamic modification of the functional connectivity between the sampled neurons. This interpretation poses several difficulties to theoreticians and experimentalists since it requires re-evaluation of most of the rate code models. In particular puzzling is the findings that the amount of correlation may change in relation to behavioral events even if the firing rate of the two neurons (their PSTs) seems to remain constant (Fig. 4).

Many neurons however, show modulation of firing rates in relation to behavioral events. In these cases, it is still possible that the modulation of the amount of excess of coincidences depends on the individual firing rates of the two neurons. If so, it is predicted that excess of coincidences is positively correlated with the modulations of the firing rates of the two neurons. This is not the case in the examples of Figs 5 where the PSTs of the two neurons are not flat; The three neurons (0, 1, 6) exhibit moderate modulation of their firing rates in relation to saccade initiation. However, it is evident that the changes of correlations could not be predicted from the firing rates of the two neurons. While the correlations either increased (4A), or decreased (4C) near the time of saccade initiation, the firing rates of both neurons was increased around the onset of saccades, regardless of its direction. To quantify and generalize the above qualitative description, we tested to what extent can one predict the temporal pattern of the correlation between two neurons from their PST histograms. To do that, we first computed the “*predicted diagonal*” (the set of *PST-predictor* bins which lie along the principle diagonal of the JPST matrix). We then, estimated the amount of similarity between the predicted-diagonal and the CTH (the normalized coincidence time histogram) that depicts the excess of coincidences. For each

such pair of diagonals (predicted vs. CTH) we computed one correlation coefficient (CC). We calculated the C.C.'s for 171 of the JPST histograms in which we found excess of coincidences. The distribution of CC's is shown in Fig. 7A.

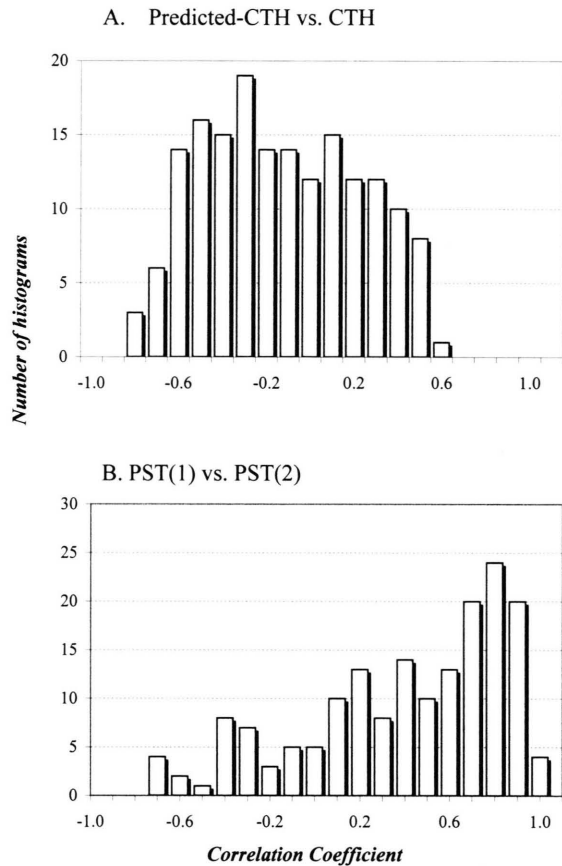


Fig. 7. Distributions of correlation coefficients for pairs of histograms. A population of 171 neuronal pairs was used in this analysis. All these pairs had a positive peak in their time averaged crosscorrelogram. A: The distribution of correlation coefficients of 171 pairs of histograms, comparing (for each neuronal pair) the predicted coincidences time histograms (Pred-CTH) to the normalized CTH. The correlation coefficients are distributed around 0 (mean -0.13 and median -0.2) indicating that the pattern of dynamic modulations of excess of coincidences (CTH) of firings of most neuronal pairs can not be predicted from modulation of their firing rates. B: The distribution of correlation coefficients comparing the patterns of PSTs of each pair of neurons. (PST(1) vs. PST(2)). Here, the distribution is skewed towards high values (mean $+0.4$, median $+0.5$), indicating that the PSTs of correlated neuronal pairs tend to be of a similar shape.

The CC values encompass a wide range. For some neuronal pairs we found that the shapes of the predicted-diagonal and the CTH were very similar (high positive CC). In these cases, there is a strong correlation between the firing rate modulations (responses) of the two neurons and the dynamics of excess correlation between them. For others, there is negative CC, indicating (surprisingly?) that the modulation of interaction between the neurons can be inversely correlated to the modulation of their firing rates. (for example – the level of coincidences may increase, while the firing-rates may decrease). For most neuronal pairs, however, the CC values are very small. The mean value is near zero and even slightly negative (mean = -0.13 , median = -0.2). To conclude, this analysis indicates that the CTH may change sometimes in the same direction as the firing rates, sometimes in the opposite direction, and more often with no relation to it.

For comparison, we also computed the CC for the pairs of peri-stimulus time histograms of the same 171 neuronal pairs. Here, the results differ markedly. Most of pairs had positive CC, as can be seen in Fig. 7B (mean $+0.4$, median 0.5). This result indicates that neurons that were recorded simultaneously, and also had positive peaks in their crosscorrelograms, tend to share similar patterns evoked changes of their firing rate in relation to the trigger event.

In conclusion: Comparison of the two distributions in Figs 7A and 7B clearly indicates that while it is possible to predict the firing rate of one neuron on the basis of the firing rate of another, it is **not** possible to predict the dynamics of their coherent spikes firings from their (similar) PSTs. Thus, we hold that patterns of the coincidence time histograms represent the modulation-patterns of inter-neuronal interactions, rather than some by-product of firing rate modulations.

In conclusion: The results presented in this section strongly suggest that excess coincidences do not evolve by modulation of the neurons firing rate. We maintain therefore, that the attractive alternative is, in fact, to venture beyond single neuron rate coding, and to incorporate the modulation of inter-neuronal interactions as a mechanism to dynamically assemble neurons into functional groups.

Discussion

The results of this study demonstrate that cortical neurons may exhibit rapid modulations of discharge correlation in relation to behavioral events. These modulations may switch the neurons firing from being incoherent into a coherent state of joint synchrony. Alternatively, the modulation may enhance temporal segregation of the neurons firing (increase of negative correlation). Each state may last from a few tens of milliseconds to several seconds. The observed modulations may be, but are not necessarily associated with changes in the individual neurons firing rates. Similar dynamics of transitions between quasi-stationary states were observed when the same data was analyzed as hidden Markov process in which transitions between states were assumed to be expressed by concomitant changes in the firing rates of several neurons (Abeles *et al.*, 1995; Seidemann *et al.*, 1996). The transitions described by the hidden-markov model (HMM), were also related to behavioral events. Further, although the states were determined on the basis of the firing rates of the neurons, it was found that the crosscorrelations between pairs of neurons was state-dependent.

Taken together these findings support the notion that a single neuron can intermittently participate in different computations by rapid changes of its coupling to other neurons, thus switching its allegiance from one functional group to another.

Previous correlation studies concentrated on relatively precise coincidences with jitters of only a few milliseconds (e.g. Toyama *et al.*, 1981; Ts'o *et al.*, 1986), the assumed jitters of direct synaptic interactions. In this paper we chose to describe the phenomenon of loose synchrony and, thus, used relatively large bins. Precise coincidences do occur, however, in the present data, as was discussed elsewhere (Abeles *et al.*, 1993). For example, JPST-analysis of the same data as in Fig. 4A, but using a narrower bin of 5 milliseconds revealed that the modulation depth of precise coincidences (with jitters of only 2.5 ms) reached values up to 620%. The wide peaks and troughs (tens to hundreds of milliseconds wide), indicate that the time-constraints of the processes evoking these correlations are loose. Such correlations (including precise coincidences) could emerge by repeated volleys of direct synaptic interactions between the

two neurons or, more likely, by a change in the pattern of activity of a large number of neurons interacting in a correlated manner with the two sampled neurons. Thus, the modifications of correlation between the two neurons reveal changes in the organization of spike activity in larger groups of neurons in relation to stimulation and behavior. Moreover, our results indicate that these groups are not randomly organized. Most pairs of neighboring neurons exhibited selective, rapid increases of positive correlation near behavioral events, whereas distant neuron pairs frequently showed compound patterns of correlation with enhancement of predominantly negative correlation near the behavioral events. These findings support and extend several anatomical and physiological findings, which indicated that functional groups are organized in clusters (Ts'o *et al.*, 1986; Eckhorn *et al.*, 1988; Selemon and Goldman-Rakic, 1990). Our findings further suggest that neighboring neurons tend to share common inputs of the same sign (either inhibitory or excitatory) whereas the effects on more distant neurons (in our study: about 500–1000 microns apart) are mixed. Therefore, when the common drive is increased, neighboring neurons tend to be activated in unison, and can operate as a coherent functional group for a short while. On the other hand, the negative correlation between neurons in one group and those in another, more distant one can accentuate the separation among groups. Thus, the spatiotemporal organization of activity in the network allows for rapid association of neurons into a functional group, at the same time dissociating such a group from concurrently-activated, competing groups. Previous modeling studies demonstrated that similar dynamic organization can indeed be accomplished in large networks, even without associated modifications of the synaptic weights (Aertsen and Preissl, 1991; Aertsen *et al.*, 1994; see also Kaneko, 1990; Hansel and Sompolinsky, 1992). Thus, dynamic modulation of firing coherence can facilitate the functional reorganization of the anatomical network according to the instantaneous computational demands. The structural properties

of the network that enhance the manifestation of dynamic functional coupling are the following: 1. sparse and weak connectivity in a very large network, 2. low average activity, 3. structured connectivity that favors excitatory connections within a number of subgroups of neurons (assemblies), 4. a spike generating mechanism that requires several (near-) coincident inputs to produce a spike. These properties are well compatible with the anatomy and physiology of the cerebral cortex and with the idea of Hebbian learning of cell assemblies. The “dynamic cell assemblies” has to be viewed as complex spatiotemporal structures of neuronal activity, consisting of many synchronously firing local subgroups, where only a fraction of the active neurons play a role as “an assembly” at any given moment (i.e. within a few to one hundred milliseconds time window). This spatiotemporal concept of the cell assembly is thereby a natural and efficient computation tool and is consistent with the known physiological mechanisms and anatomical constraints. Repeated occurrences of dynamic co-activation of the kind described here may have additional, more lasting implications. There is ample evidence that repeated co-activation of neurons may lead to enhancement of specific functional circuits by Hebb-like mechanisms for synaptic modification (Kelso *et al.*, 1986; Gustafsson *et al.*, 1987; Fregnac *et al.*, 1988; Bonhoeffer *et al.*, 1989; Ahissar *et al.*, 1992b). As a result, repeated ignition of functional neuron groups will leave traces in the connectivity of the neural network, thereby paving the way for rapid and reliable traversal on future occasions. Hence, dynamic modulation of firing coherence can facilitate learning by supporting the process of reorganizing the network, thereby enabling the organism to improve performance and acquire skill.

Acknowledgments

The study was supported in part by grants from the *Israeli Academy of Sciences and Humanities* and the *American-Israel Bi-national Science Foundation (BSF)*.

- Abeles M. (1982), Local Cortical Circuits. An Electrophysiological Study. Springer, Berlin.
- Abeles M. (1991), Corticonics. Neural Circuits in the Cerebral Cortex. Cambridge University Press, Cambridge, UK.
- Abeles M., Bergman H., Margalit E. and Vaadia E. (1993a), Spatiotemporal firing patterns in the frontal cortex of behaving monkeys. *J. Neurophysiol.* **70**, 1629–1643.
- Abeles M., Prut Y., Bergman H., Vaadia E. and Aertsen A. (1993b), Integration, synchronicity and periodicity. In: *Brain Theory: Spatiotemporal Aspects of Brain Function* (Aertsen A., ed.). Elsevier Science Publ., Amsterdam, pp. 149–181.
- Abeles M., Bergman H., Gat I., Meilijson I., Seidmann E., Tishby N. and Vaadia E. (1995), Cortical activity flips among quasi-stationary states. *Proc. Natl. Acad. Sci.* **92**, 8616–8620.
- Allum J. H., Hepp Reymond M. C. and Gysin R. (1982), Cross-correlation analysis of interneuronal connectivity in the motor cortex of the monkey. *Brain Res.* **231**, 325–334.
- Aertsen A. M. H. J., Gerstein G. L., Habib M. K. and Palm G. (1989), Dynamics of neuronal firing correlation: modulation of “effective connectivity”. *J. Neurophysiol.* **61**, 900–917.
- Aertsen A. and Preissl H. (1991), Dynamics of activity and connectivity in physiological neuronal networks. In: *Nonlinear Dynamics and Neuronal Networks* (Schuster H., ed.). VCH Verlag, Weinheim, pp. 281–301.
- Aertsen A., Erb M. and Palm G. (1994), Dynamics of functional coupling in the cerebral cortex: An attempt at a model-based interpretation. *Physica D* **75**, 103–128.
- Ahissar M., Ahissar E., Bergman H. and Vaadia E. (1992a), Encoding of sound-source location and movement: activity of single neurons and interactions between adjacent neurons in the monkey auditory cortex. *J. Neurophysiol.* **67**, 203–215.
- Ahissar E., Vaadia E., Ahissar M., Bergman H., Arieli A. and Abeles M. (1992b), Dependence of cortical plasticity on correlated activity of single neurons and on behavioral context. *Science* **257**, 1412–1415.
- Arieli A., Shoham D., Hildesheim R., Grinvald A. (1995), Coherent spatiotemporal patterns of ongoing activity revealed by real-time optical imaging coupled with single-unit recording in the cat visual cortex. *J. Neurophysiol.* **73**(5), 2072–2093.
- Barlow H. B. (1972), Single units and sensation: a neuron doctrine for perceptual psychology? *Perception* **1**, 371–394.
- Barlow H. B. (1992), Single cells versus neuronal assemblies. In: *Information Processing in the Cortex: Experiments and Theory* (Aertsen A. and Braitenberg V. B., eds.). Springer, Berlin, pp. 169–174.
- Bonhoeffer T., Staiger V. and Aertsen A. (1989), Synaptic plasticity in rat hippocampal slice cultures: local ‘Hebbian’ conjunction of pre- and postsynaptic stimulation leads to distributed synaptic enhancement. *Proc. Natl. Acad. Sci.* **86**, 8113–811.
- Bienenstock E. and German S. (1993), Compositionality in neural systems. In: *The Handbook of Brain Theory and Neural Networks* (Arbib, ed.).
- Braitenberg V. (1978), Cell assemblies in the cerebral cortex. In: *Theoretical Approaches to Complex Systems*. Lecture Notes in Mathematics, Vol. **21** (Heim R. and Palm G., eds.). Springer, Berlin, Heidelberg, New York, 171–188.
- Braitenberg V. and Schüz A. (1991), *Anatomy of the Cortex. Statistics and Geometry*. Springer, Berlin.
- Desmedt J. E. and Tomberg C. (1994), Transient phase-locking of 40 Hz electrical oscillations in prefrontal and parietal human cortex reflects the process of conscious somatic perception. *Neurosci. Lett.* **168**, 126–129.
- Eckhorn R., Bauer R., Jordan W., Brosch M., Kruse W., Munk M. and Reitboeck H. J. (1988), Coherent oscillations: a mechanism of feature linking in the visual cortex? Multiple electrode and correlation analysis in the cat. *Biol. Cybern.* **60**, 121–130.
- Engel A. K., Kreiter A. K., König P. and Singer W. (1991), Interhemispheric synchronization of oscillatory responses in cat visual cortex. *Science* **252**, 1177–1179.
- Fetz E., Toyama K. and Smith W. (1991), Synaptic interactions between cortical neurons. In: *Cerebral Cortex*, Vol. **9** (Peters A., ed.). Plenum Publ., New York, pp. 1–47.
- Fregnac Y., Shulz D., Thorpe S. and Bienenstock E. (1988), A cellular analogue of visual cortical plasticity. *Nature* **333**, 367–370.
- Gerstein G. L. and Perkel D. H. (1969), Simultaneously recorded trains of action potentials: analysis and functional interpretation. *Science* **164**, 828–830.
- Georgopoulos A. P., Schwartz A. B. and Kettner R. E. (1986), Neuronal population coding of movement direction. *Science* **233**, 1416–1419.
- Georgopoulos A. P., Lurito J. T., Petrides M., Schwartz A. B. and Massey J. T. (1989), Mental rotation of the neuronal population vector. *Science* **243**, 234–236.
- Gerstein G. L., Perkel D. H. (1972), Mutual temporal relationships among neuronal spike trains. *Biophys. J.* **12**, 453–473.
- Gray C. M. and Singer W. (1989), Stimulus-specific neuronal oscillations in orientation columns of cat visual cortex. *Proc. Natl. Acad. Sci. USA* **86**, 1698–1702.
- Gray C. M., Engel A. K., König P. and Singer W. (1992), Synchronization of oscillatory neuronal responses in cat striate cortex: temporal properties. *Vis. Neurosci.* **8**(4), 337–47.
- Gustafsson B., Wigström H., Abraham W. C. and Huang Y. Y. (1987), Long term potentiation in the hippocampus using depolarizing current pulses as the conditioning stimulus to single volley synaptic potentials. *J. Neurosci.* **7**, 774–780.
- Hansel D. and Sompolinsky H. (1992), Synchronization and computation in chaotic neural network. *Phys. Rev. Lett.* **68**, 718–724.
- Hebb D. (1990), *The Organization of Behavior. A Neuropsychological Theory*. Wiley, New York.
- Kaneko K. (1990), Clustering, coding, switching, hierarchical ordering, and control in a network of chaotic elements. *Physica D* **41**, 137–172.
- Kelso S. R., Ganong A. H. and Brown T. H. (1986), Hebbian synapses in hippocampus. *Proc. Natl. Acad. Sci. USA* **83**, 5326–5330.
- Krüger J. and Aiple F. (1988), Multimicroelectrode investigation of monkey striate cortex: spike trains correlations in infragranular layers. *J. Neurophysiol.* **60**(2).

- Krüger J. (1990), Multi-microelectrode investigation of monkey striate cortex: link between correlational and neuronal properties in the infragranular layers. *Vis. Neurosci.* **5**, 135–142.
- Kwan H. C., Murphy J. T. and Wong Y. C. (1987), Interaction between neurons in precentral cortical zones controlling different joints. *Brain Res.* **400**, 259–269.
- Lukashin A. V. and Georgopoulos A. P. (1993), A dynamical neural network model for motor cortical activity during movement: population coding of movement trajectories. *Biol. Cybern.* **69**, 517–524.
- Moore G. P., Segundo J. P., Perkel D. H. and Levitan H. (1970), Statistical signs of synaptic interaction in neurons. *Biophys. J.* **10**, 876–900.
- Murthy V. N., Aoki F. and Fetz E. E. (1994), Synchronous oscillations in sensorimotor cortex of awake monkeys and humans. In: *Oscillatory Event Related Brain Dynamics* (Porter C., Elbart T. and Lutkenhoner B., eds.), Plenum Publishing Corp.
- Murthy V. N. and Fetz E. (1996), Synchronization of neurons during local field potential oscillations in sensorimotor cortex of awake monkeys. *J. Neurophys.* **76**(6), 3968–3982.
- Nelson J. I., Salin P. A., Munk M. H., Arzi M. and Bullier J. (1992), Spatial and temporal coherence in cortico-cortical connections: a cross-correlation study in areas 17 and 18 in the cat. *Vis. Neurosci.* **9**, 21–37.
- Palm G., Aertsen A. M. H. J. and Gerstein G. L. (1988), On the significance of correlations among neuronal spike trains. *Biol. Cybern.* **59**, 1–11.
- Palm G. (1993), On the internal structure of cell assemblies. In: *Brain Theory: Spatiotemporal Aspects of Brain Function* (Aertsen A., ed.), Elsevier Science Publ., Amsterdam, pp. 261–270.
- Perkel D. H., Gerstein G. L. and Moore G. P. (1967), Neuronal spike trains and stochastic point processes. II. Simultaneous spike trains. *Biophys. J.* **7**, 419–440.
- Press W. H., Flannery B. P., Teukolsky S. A. and Vetterling W. T. (1988), *Numerical Recipes in C: The Art of Scientific Computing*. Cambridge University Press, pp. 60–72.
- Roelfsema R. P. (1998), Solutions to the binding problem. *Z. Naturforsch.* **53c**, 691–715.
- Rotter S. and Aertsen A. (1998), Accurate spike synchronization in cortex. *Z. Naturforsch.* **53c**, 686–690.
- Richmond B. J. and Optican L. M. (1987), Temporal encoding of two-dimensional patterns by single units in primate inferior temporal cortex. II. Quantification of response waveform. *J. Neurophysiol.* **57**, 147–161.
- Salinas E. and Abbott L. F. (1994), Vector reconstruction from firing rates. *J. Comp. Neurosci.* **1**, 89–108.
- Schwartz A. B. (1993), Motor cortical activity during drawing movements: population representation during sinusoid tracing. *J. Neurophysiol.* **70**, 28–36.
- Schwartz A. B. (1994), Direct cortical representation of drawing. *Science*. **265**, 540–542.
- Schillen T. B. and König P. (1994), Binding by temporal structure in multiple feature domains of an oscillatory neuronal network. *Biol. Cybern.* **70**, 397–405.
- Sanes J. N. and Donoghue J. P. (1993), Oscillations in local field potentials of the primate motor cortex during voluntary movement. *Proc. Natl. Acad. Sci. USA* **90**, 4470–4474.
- Selemon L. D., Goldman Rakic P. S. (1990), Topographic intermingling of striatonigral and striatopallidal neurons in the rhesus monkey. *J. Comp. Neurol.* **297**, 359–376.
- Seidemann E., Meilijson I., Abeles M., Bergman H. and Vaadia E. (1995), Simultaneously recorded single units in the frontal cortex go through sequence of discrete and stable states in monkeys performing a delayed localization task. *J. Neurosci.* **16**(2), 752–768.
- Seung H. S. and Sompolinsky H. (1993), Simple models for reading neuronal population codes. *Proc. Natl. Acad. Sci. USA* **90**, 10749–10753.
- Smith W. S. and Fetz E. E. (1989), Effects of synchrony between primate corticomotoneuronal cells on postspike facilitation of muscles and motor units. *Neurosci. Lett.* **96**, 76–81.
- Sparks D. L., Holland R. and Guthrie B. L. (1976), Size and distribution of movement fields in the monkey superior colliculus. *Brain Res.* **113**, 21–34.
- Toyama K., Kimura M. and Tanaka K. (1981), Crosscorrelation analysis of interneuronal connectivity in cat visual cortex. *J. Neurophysiol.* **46**, 191–201.
- Ts'o D. Y., Gilbert C. D. and Wiesel T. N. (1986), Relationships between horizontal interactions and functional architecture in cat striate cortex as revealed by cross-correlation technique. *J. Neurosci.* **6**, 1160–1170.
- Vaadia E. and Aertsen A. (1992), Coding and computation in the cortex: single-neuron activity and cooperative phenomena. In: *Information Processing in the Cortex: Experiments and Theory* (Aertsen A. and Braitenberg V. eds.), Springer, Berlin, pp. 81–121.
- Vaadia E., Haalman I., Abeles M., Bergman H., Prut Y., Slovin H. and Aertsen A. (1995a), Dynamics of neuronal interactions in the monkey cortex in relation to behavioral events. *Nature* **373**, 515–518.
- Vaadia E., Aertsen A. and Nelken E. (1995b), 'Dynamics of Neuronal Interactions' cannot be explained by 'neuronal transients'. *Proc. B. Roy. Soc.* **26**, 407–410.
- von der Malsburg C. (1981), The correlation theory of brain function. Internal report 81-2, Max-Planck-Institute for Biophysical Chemistry, Göttingen (FRG).
- Wise S. P., di Pellegrino G. and Boussaoud D. (1996), The premotor cortex and nonstandard sensorimotor mapping. *Can. J. Physiol. Pharmacol.* **74**:4, 469–482.